Collagen fibre characterisation in arterial tissue under load using SALS

R.T. Gaul[1,2], D.R. Nolan[1,2], C. Lally[1,2]

[1]Trinity Centre for Bioengineering, Trinity College Dublin, Dublin, Ireland.

[2]School of Engineering, Trinity College Dublin, Dublin, Ireland.

Abstract

The collagen fibre architecture of arterial tissue is known to play a key role in its resultant mechanical behaviour, while maladaptive remodelling of this architecture may be linked to disease. Many of the techniques currently used to analyse collagen fibre architecture require time consuming tissue preparation procedures and are destructive in nature. The aim of this study is to fully explore Small Angle Light Scattering (SALS) as a means to non-destructively assess collagen fibre architecture in arterial tissue and subsequently gain insights into load induced reorientation.

The optimised configuration of the SALS system for arterial tissue was determined using quantitative comparisons to histological analyses of porcine carotid artery as its basis. Once established, layer specific fibre orientation and the influence of tissue loading was determined for thin sections of carotid artery using SALS. This process was subsequently repeated for intact carotid artery layers. A single family of circumferentially orientated collagen fibres were found in the intima ((-0.1±1.4° (5.5°)) and media (-1.7±1.9° (4.7°)) while two perpendicular families of fibres were identified in the adventitia (-6.4±0.7° (37.7°) and 118.3±2.7 (39.9°)). An increase in fibre alignment in response to a 20% circumferential strain was also identified using SALS, characterised by an increase in scattered light eccentricity.

Results determined using SALS agreed with those found using traditional destructive techniques, however SALS has the important benefits of allowing vessel layers to remain intact, and has a fast processing time. SALS unique ability to identify load induced reorganisation in intact arterial layers offers an efficient means to gain crucial insights into arterial disease and its development over time.

1 Introduction

Changes in the mechanical properties of arteries are believed to play a key role in arterial disease development and progression, potentially explaining the tendency for arterial disease to manifest itself in specific locations (O'Rourke, 1995). Altered fibre architectures have been identified in human aneurysmal tissue (Gasser et al., 2012; Niestrawska et al., 2016) and atherosclerotic tissue (Tsamis et al., 2013), suggesting a link between disease and maladaptive collagen fibre remodelling. This collagen fibre remodelling in turn influences tissue mechanical properties (Chai et al., 2015). Information on the detailed fibre architecture of arterial tissues and how this architecture is influenced by load is therefore central to understanding the aetiology of vascular disease (Creane et al., 2011; Ghazanfari et al., 2012).

Although histology is considered the gold standard for microstructural assessment of tissues, alternative imaging modalities are increasingly being explored to assess fibre organisation. Commonly used techniques include polarised light microscopy (PLM) (Canham et al., 1989; Sáez et al., 2016; Schriefl et al., 2012) and electron microscopy (Dahl et al., 2007; Wolinsky and Glagov, 1964); however, these techniques often require time-consuming tissue preparation steps and are destructive in nature. Consequently, non-destructive techniques such as confocal microscopy (O'Connell et al., 2008; Rezakhaniha et al., 2012) and multiphoton microscopy (Cicchi et al., 2010; Zoumi et al., 2004) are growing in popularity as they allow tissues to remain intact during imaging. Unlike confocal microscopy, multiphoton microscopy

with second harmonic generation (SHG) imaging requires no special preparation or staining of vessels. SHG imaging has previously been used to interrogate fibre orientation through a vessel thickness (Keyes et al., 2011; Watson et al., 2016) and in response to physiological and biaxial loading (Keyes et al., 2011) of mouse aortic tissue without the separation of layers. However, given the limited depth of penetration of such imaging techniques, they cannot be used for imaging the full intact wall, or even intact layers, of thicker vessel walls such as porcine carotid arteries.

The critical advantage of these non-destructive imaging methods is their ability to measure real-time changes in fibre orientation in response to load (Hu et al., 2009; Keyes et al., 2011; Voytik-Harbin et al., 2003). These methods, however, are time consuming as only highly localised regions of tissue can be interrogated, rendering the real-time quantification of tissue fibre reorganisation somewhat impracticable with multiple samples (Nierenberger et al., 2015). Advances in emerging imaging modalities such as diffusion tensor imaging (DTI) have shown great promise in determining tissue fibre orientation in intact tissue samples *ex vivo* and potentially *in vivo*. However, further development is still required, particularly given the lengthy acquisition time of such imaging methods (Flamini et al., 2015, 2013, 2010; Ghazanfari et al., 2015; Shahid et al., 2016).

Small angle light scattering (SALS) analysis may offer an alternative means of measuring fibre orientations *ex vivo* across large regions of tissue without the need for time-consuming preparation steps. In SALS, incident light is scattered orthogonally to the central axis of a sample's constituent fibres, providing details on a sample's structure. SALS also offers the potential to determine real-time structural changes in intact tissue in response to load (Robitaille et al., 2011; Sacks et al., 1997; Williams et al., 2009). Most of the work published on SALS to date has looked at thin, highly organised tissue structures, such as bovine pericardium (Sacks et al., 1994) and porcine aortic valve tissue (Billiar and Sacks, 1997; Sacks

et al., 1997); whereas, SALS has seen very limited use in characterising arterial tissue. The apparent lack of SALS based arterial fibre studies may be attributed to the thickness of arterial tissues and the complex multi-layered nature of the artery wall.

In fact, only two studies have been identified by the authors where SALS has been used for arterial fibre characterisation, namely Williams et al. (Williams et al., 2009) and Haskett et al. (Haskett et al., 2010). Williams et al. used SALS to quantify fibre orientation and fibre reorganisation in native and decellularised rabbit carotid artery. Although vessels were kept intact, glycerol treatment was required to allow adequate light transmission through the vessel wall, potentially altering vessel structure. By keeping the vessel intact, the resulting signal will also include contributions from each vessel layer, an issue if vessel architecture varies from layer to layer, this is an issue if vessel architecture varies from layer to layer which has been well established in arteries (Schriefl et al., 2012). The process of glycerol treatment as used by (Williams et al., 2009) dehydrates and clears the tissue and whilst this increases its transparency, it completely alters its stiffness and structure. This process therefore limits the use of this tissue for real time analysis of structural changes in tissue architecture in response to load, including reorientation of collagen fibres, production of new collagen fibres and the degradation of existing collagen fibres (Robitaille et al., 2011). Haskett *et al.* adopted SALS as a means of identifying changes in fibre structure based on age and anatomical location of 50 μm cryo-sectioned human aortic tissue, finding an increase in circumferential fibre frequency with age. However, very large bin sizes were used to identify these differences, with circumferential fibres classified as any fibre within 45° of the circumferential direction. To date, no study has demonstrated any degree of optimisation of the system or truly identified whether SALS can accurately identify load induced changes in the fibrous structure of arterial tissue. To allow the quantification of real-time fibre remodelling in response to load, tissue specimens should not be chemically treated before analysis using SALS (Robitaille et al.,

2011). However, both of these studies used tissue preparation approaches which fix the tissue, making quantification of real-time remodelling impossible.

The overall objective of this study is to fully explore SALS as a means of measuring fibre architecture in arterial tissue. Specifically, we wish to establish whether it can be used as a non-destructive or semi-destructive method to decipher load-induced changes in fibre structure in real-time.

2 Material and methods

2.1 Tissue harvesting

Fresh porcine common carotid arteries were excised from 15 Large White pigs aged 6 months and weighing approximately 80 kg at the time of slaughter. Carotid arteries were transported on ice and processing began within 2 hours of slaughter. The excised vessels were washed with PBS to remove residual blood, and excess connective tissue was removed. The vessels were cut into 2 adjacent tube-like sections 8 mm in length from the proximal end of the vessel. The tubes were cut open longitudinally to obtain 2 flat rectangular strips.

This dissection process removes the residual stresses present within the vessel *in vivo* and consequently, may result in a more undulated collagen fibre architecture. In order to reduce the risk of recording fibre undulation rather than orientation in later analysis, specimen were gently squeezed between two slides consistent with other studies on such tissue (Gasser et al., 2012; Sáez et al., 2016).

In the present study full intact intimal, medial, and adventitial layers are analysed. To obtain intact vessel layers, an incision was first made in the vessel cross section at the layer boundary under a microscope. Next, the vessel layers were carefully separated using a rolling and peeling technique with a forceps (Holzapfel et al., 2007). Only vessels with medial layers

with a thickness below 600 μm (0.545±0.045 μm) were chosen to ensure sample consistency. Additionally, thin histological sections of each layer were analysed.

2.2 Histological processing

All histological samples were fixed in 4% paraformaldehyde overnight, dehydrated in a graded series of ethanol baths (EtOH), cleared in xylene before being embedded in paraffin wax. The resulting paraffin embedded samples were sectioned at 8 μm using a microtome (RM-2125RT, LEICA, Germany) and affixed to microscope slides. A minimum of 2 sections were obtained from each of the 3 vessel layers for staining (108 slices in total).

The resulting sections were stained with picrosirius red to assess collagen fibre distribution. Although collagen fibres are naturally birefringent, picrosirius red significantly enhances this property without negatively impacting perceived fibre orientation under polarised light.

2.3 Loading

To identify changes in fibre orientations due to loading, a nominal strain of 20% was applied to one sample arising from each vessel. For histological sections, samples were strained and pinned to a mounting plate before being fixed in 4% paraformaldehyde overnight; this allowed further histological processing of the sample in its loaded state (Figure 1). Once fixed, the mounting pins were removed and the tissue dehydrated, cleared and wax embedded as outlined in Section 2.2 above. For intact layer samples, strain was applied using a custom device mounted inside the SALS system.

2.4 SALS system setup

An in-house SALS system was built, based on an existing system described in the literature (Sacks et al., 1997). This set-up consists of: an unpolarised 5 mW HeNe laser (λ = 632.8 nm; JDSU, Newbury, UK), focussing lenses (various focal lengths; Edmund Optics Ltd, York, UK),

automated sample positioner, projection screen and a CMOS USB camera. Each component is mounted on a guide rail, to enable fine linear positional adjustments (Figure 2A).

In order to obtain the desired beam diameter, the antagonising laser light is passed through different lens configurations before encountering the specimen, which is held in an automated positioning and stretching device (Figure 2B). A camera records the resulting scattered light pattern as it is projected onto a semi-transparent HDPE projection screen.

The specimen positioning device consists of 2 linear traverses, allowing travel in both x and y directions. Each linear traverse is coupled to a stepper motor (200 steps/revolution; Pololu Corporation, Las Vegas, NV, USA), providing a linear movement resolution of 5 μm across the system's 30 mm range. Stepper motor control and image acquisition are controlled through a custom LabVIEW programme (National Instruments, Berkshire, UK), which allows the user to specify the region of interest in a sample and the interrogation point spacing (see Figure 3A). An image of the scattered light pattern is taken and saved at each interrogation point as a sample is raster scanned. The fibre orientation at each of these points is subsequently determined by post-processing these recorded images. Whilst SALS measurement speed is influenced by the user defined parameters used, in this study each test specimen imaged included 192 interrogation points across a 4 x 3 mm region of interest which takes approximately 4 minutes to scan.

2.5 Orientation analyses

2.5.1 Histological orientation analysis (HOA)

Images of histological sections were taken under crossed polarisers at two polarising angle configurations, 45° apart, using an Olympus BX-41 microscope equipped with a QImaging MicroPublisher 5.0 RTV camera. The resulting images are overlaid to achieve a complete picture of collagen fibre orientation in a sample (Figure 4).

Histological orientation analysis (HOA) was carried out at the same interrogation region as SALS measurements across several thin histological sections. Fibre distributions are determined by identifying pixel gradients in each image using the OrientationJ plugin (Rezakhaniha et al., 2012) for ImageJ (Schneider et al., 2012). Mean fibre orientation and fibre distributions were determined and compared to those determined using SALS, allowing the identification of the most suitable SALS system configuration for arterial tissue.

2.5.2 SALS analysis

The scattering pattern was automatically analysed using a purpose built Matlab (MathWorks, Cambridge, UK) code allowing for predominant collagen fibre orientations to be determined. The code determines the centroid of the scattered light pattern before systematically cycling through all angles from 1° to 360°, computing the light intensity at each angle (Figure 3 B-C). Light scatters orthogonally to a fibre's axis, hence the dominant fibre orientation at a specific location can be calculated. Each sample is raster scanned over the region of interest and the fibre direction at each point is calculated.

The scattered light forms an elliptical shape with eccentricity, E, which indicates the distribution of fibres at a given interrogation point. Eccentricity is based on the ratio of major and minor axes and is given as,

$$\mathrm{E} = 2\frac{\sqrt{\left(\frac{\text{Major Axis}}{2}\right)^2 - \left(\frac{\text{Minor Axis}}{2}\right)^2}}{\text{Major Axis}} \quad (1)$$

An eccentricity of 1 corresponds to perfect fibre alignment in one direction only, while a value of 0 corresponds to an isotropic distribution of fibres. Using both fibre orientation and alignment, structural differences and responses to load can be identified.

2.5.3 Statistics

Statistical analysis of fibre distributions for both SALS and HOA was carried out using a circular statistics toolbox for Matlab (Berens, 2009) and GraphPad Prism 6.0 (GraphPad Software, CA, USA). Normality of distributions was tested using D'Agostino-Pearson normality test. Correlation coefficients were calculated based on the difference in normalised orientation distributions between SALS and HOA at each angle across each sample. Fibre families in adventitial samples were determined using k-means clustering for circular data (Berens, 2009). Changes in eccentricity in response to strain for the three distinct layers of the artery were analysed using unpaired t-tests, while unbalanced one-way ANOVA was used for all other comparisons. Differences were considered significant when $P < 0.05$. All HOA and SALS measurements were measured relative to the circumferential direction ($\theta = 0°$). Results are expressed as mean±standard error (standard deviation).

2.6 SALS optimization

One of the primary objectives of the current study was to determine the optimum SALS system configuration for analysing arterial tissue. HOA was first performed using different interrogation region areas to determine whether there is important small-scale fibre distribution detail that SALS may be insensitive to. Next, SALS was performed on thin histological samples using three different beam diameters and three different interrogation point spacings. Results were compared with fibre orientations found using HOA at the same interrogation points to identify the most accurate configuration. To investigate whether fibre distributions change at different scales, interrogation region areas of 600 μm^2, 150 μm^2 and 75 μm^2 were chosen, corresponding to the SALS beam diameters investigated. Furthermore, an interrogation region of 35 μm^2 was used to detect any small-scale fibre distributions. A laser beam diameter of 600 μm was previously used for bovine tendon (Sacks et al., 1997) and is used here, additionally

beam diameters of 150 µm and 75 µm were also tested. Interrogation point spacings of 75 µm, 125 µm and 250 µm were investigated.

3 Results

3.1 SALS system optimisation

3.1.1 Small Scale fibre distributions determined from histology

HOA results showed no important small scale fibre orientation or distribution differences for the intima and media layers (Figure 5A). However, the fibre angle distribution tended to narrow and become noisier as the interrogation region reduced in size. In contrast, in the adventitial layer there was greater variation in fibre distribution observed as interrogation region varied in size (Figure 5B).

These results show that in the intima and medial layers there is little loss of information if a large interrogation region is utilised. The fibre orientation distribution measured in the adventitial layer does change in response to a change in the interrogation region size. However, the change is not substantial and can be attributed to the undulating fibre structure of the adventitia (see Figure 4C).

3.1.2 Optimum SALS beam diameter

The mean fibre orientation measured using SALS for 3 different beam diameters is compared to that measured using HOA at the same interrogation point. Figure 6A plots the error in degrees between SALS and HOA and shows that a beam diameter 150 µm results in the lowest error across all 3 vessel layers (I: 2.6±0.5° (1.6°), M: 3.3±0.5° (1.6°), A: 9.5±2.7° (8.5°)). Circular statistics based on the results of HOA demonstrate significant differences between the adventitial layer and the medial and intimal layers (Figure 6B). In addition to closely identifying mean fibre orientation, similar fibre distributions were determined using SALS and

HOA at the same interrogation region (Figure 7A). This observation was seen quantitatively through the high correlation between fibre distributions across each layer (Figure 7B).

3.1.3 Optimum SALS interrogation spacing

Moving forward with a beam diameter of 150 μm, the effect of interrogation point spacing for each arterial layer was analysed. Figure 8 shows that spacing has little effect on the mean orientation of a sample, for both the intimal and medial layers.

No statistical difference was found in mean fibre orientation for interrogation spacings of 75 μm, 125 μm and 250 μm (Figure 8). However, mean orientation showed greater variation based on the interrogation spacing chosen for the adventitia.

3.2 Analysis of thin sections

Figure 9A and B plot the results of a SALS analysis on a full sample, showing the mean fibre orientation at multiple interrogation points in the region of interest. The eccentricity in the plots qualitatively indicate fibre distribution in the sample. SALS was also capable of measuring regions of considerable fibre reorganisation observed in loaded tissues occurring around the pins (Figure 9C). This reorganisation was also observed in a histological image, and was quantified using HOA (Fomovsky and Holmes, 2010) (Figure 9D).

3.2.1 Unloaded tissue

Polar histogram plots of all data show a single circumferential (0°) fibre distribution for unstrained intima (-0.1±1.4° (5.5°)) and media (-1.7±1.9° (4.7°)) thin sections (Figure 10A i-ii). In contrast, a more complex multi-directional structure was identified in the adventitial layer with single and multiple fibre populations. Two fibre populations were identified using k-means clustering for circular data, with mean angles of -6.4±0.7° (37.7°) and 118.3±2.7 (39.9°) (Figure 10A iii)

3.2.2 Loaded tissue

Circumferential strain had minimal influence on mean fibre orientation due to the existing circumferential orientation of fibres (Figure 10A iv-vi). While small changes occur in mean fibre orientations due to strain (Figure 9A-B), a 7.4% and 5.7% increase in eccentricity was seen for intimal and medial tissue respectively (Figure 10B).

3.3 Analysis of intact vessel layers

Having analysed thin histological sections of arterial wall, SALS analysis was applied to intact vessel layers. Polar histogram plots of fibre distribution show similar distributions to our thin slice results for intima (-2.3±1.9° (4.7°)), media (-2.7±1.2° (3.2°)) and adventitia (-1.4±3.5° (8.5°)), see Figure 10C. However, analysis of intact layers did not identify a second axial population of adventitial fibres as seen previously. The mean fibre orientations measured using SALS were also observed using SHG imaging (see supplementary data). Similar increases in eccentricity were also observed in intact intimal and medial layers in comparison to SALS of histological sections in response to a 20% strain (Figure 10B).

4 Discussion

The goal of this study was to establish whether SALS is capable of repeatedly and reproducibly characterising collagen fibre orientation in arterial tissue and how this architecture changes in response to load. To achieve this, the SALS system was first optimised for use with arterial tissue before an analysis of thin arterial sections and intact vessel walls was performed. A predominant circumferential fibre orientation was found in both thin vessel slices and intact vessel layers, while a second less dominant axial fibre family was identified in the adventitia. SALS was also capable of identifying decreased fibre dispersion in response to vessel loading, through an increase in eccentricity. These results indicate that SALS is a

quick and objective alternative to histology for fibre orientation analysis of arterial tissue, with the potential to offer insights into real-time fibre remodelling in intact tissue.

4.1.1 Beam Diameter

A beam diameter of 150 μm was chosen as the optimum for arterial tissue based on quantitative comparisons made with accepted histological results (Figure 6A). This is the first instance in which beam diameter has been optimised for arterial tissue. Reducing the beam diameter further to 75 μm resulted in an increase in system noise caused by self-interference of the scattered light, as noted elsewhere (Sacks et al., 1997). The relatively higher angular error found for adventitial measurements was attributed to the more complex, undulated fibre structure observed histologically (Figure 4C).

4.1.2 Interrogation Point Spacing

Due the high alignment, low dispersion fibre structure of the intimal and medial layers, interrogation point spacing has little effect on the mean fibre angle measured. In contrast, in adventitial samples there is a considerable difference in the mean fibre angle measured at a spacing of 250 μm. For this spacing distance the beam diameters do not overlap, unlike the two lower spacing distances. The non-contribution of these unmeasured regions to the mean angle may account for this difference. The interrogation point spacing should ultimately be chosen based on which layer is be examined, the size of the region of interest, and the level of detail required (Figure 9A-C).

4.1.3 Fibre orientation

A single family of circumferentially orientated collagen fibres was identified in the intima and media of porcine carotid artery (Figure 10A). This result is in keeping with previous studies of the carotid artery using PLM (Sáez et al., 2016) and DTI (Shahid et al., 2016), however it differs from the typical multifamily structure observed in human aortic vessels (Gasser et al.,

2012; Schriefl et al., 2012). This study has considered layer specific fibre orientations and found there is a different fibre structure in the adventitia, with two fibre families identified. This contrasts results from Saez *et al.* (Sáez et al., 2016) who concluded there was a single fibre family in the carotid artery. That study used PLM of 3 histological slices taken at non-specified depths through the carotid artery wall and may have omitted the adventitial layer completely. Previous studies on the common iliac artery using layer specific PLM have determined a single family of fibres in the intima and media, and two families in the adventitia (Schriefl et al., 2012). It has been suggested that the relatively low level of axial strain in common iliac arteries is one reason for this single family fibre structure in the media (Qi et al., 2015). These fibre architecture differences underscore the necessity of investigating specific vessel layers, locations and mechanics.

Collagen orientation under loading was calculated to determine whether SALS has the sensitivity to identify structural changes in intact layers, an important consideration if further real time remodelling analysis is to be carried out (Gaul and Lally, 2017). Circumferential strain applied to the vessel resulted in a slight shift in mean fibre orientation of the already near circumferentially aligned fibres (Figure 10A). Circumferential strain also led to increased fibre alignment, identified by SALS through an increase in scatted light eccentricity in intimal and medial layers. The unexpected reduction in eccentricity seen in adventitial tissue may be attributed to increased disorganisation in its multi-family fibre architecture. These changes in eccentricity highlight SALS ability to capture dispersion information of collagen fibres, something which is often incorporated into mathematical models of the arterial wall (Gasser et al., 2006; Sacks, 2003).

SALS was also capable of measuring a similar predominant circumferential fibre distribution in intact vessel layers (Figure 10C). This study is the first to analyse intact arterial tissue using SALS without glycerol clearing to increase transparency (Williams et al., 2009).

While glycerol treatment allows the entire vessel wall to remain intact, the chemical treatment prevents real time reorganisation or remodelling of collagen fibres to be analysed in a realistic way. The argument to separate a vessel into distinct layers before SALS testing is strengthened by the confirmation that a different fibre architecture exists in the adventitia, which may obscure results were the vessel to be kept fully intact. Indeed, preliminary SALS testing of glycerol treated full vessel arteries exhibited different scattered light patterns depending on whether the adventitia faced toward or away from the incoming laser light (see supplementary material). These differences arose in response to bias imposed by the layer which the light passes through last, which has the greatest influence on the light scattering. Moreover, layer separation allows one to analyse layer specific reorientation and remodelling in real time and under load. SALS fibre measurements made on intact layers agree with SALS results for thin histological sections of the intima and media. However, the more complex multi-family fibre structure observed in thin histological sections of the adventitia using SALS was not observed in intact layers. It is plausible that the dominant circumferential fibre family seen in the adventitia may mask the less dominant second axial fibre family when intact layers are analysed using SALS.

4.1.4 Benefits of SALS

SALS offers many advantages over existing techniques used in characterising fibre orientations of soft tissues with its ability to quickly and objectively measure fibre orientations over large regions with minimal pre-processing. SALS can effectively analyse large tissue regions in a number of minutes, compared to hours for SHG imaging, and days for histological imaging of similar size regions. SALS greatest strength, however, is its potential to look at real time reorganisation and remodelling of intact tissue which until now has yet to be investigated in arterial tissue. The existence of a load-sensitive protective mechanism for collagen fibres has previously been identified in corneal tissue (Robitaille et al., 2011), bovine pericardium

(Ellsmere et al., 1999; Ghazanfari et al., 2016) and rat tail tendon (Wyatt et al., 2009), yet it remains to be seen whether this mechanism exists in arteries. SALS ability to non-destructively assess structural changes in intact arterial layers can aid in deciphering whether a load dependent degradation mechanism exists, and how this mechanism may influence healthy and diseased vessel remodelling.

4.1.5 Study limitations

It is worth noting that SALS is limited by the transparency of the sample to be interrogated. With this, thin, histological slices of tissue are not an issue; however, issues may arise as sample thicknesses increase. Additionally, as sample thickness increases, multiple scattering of light by fibres through a sample's thickness may obscure results. As layer thickness increased, the signal to noise ratio reduced and the predominate fibre directions were difficult to ascertain from the light scattering pattern resulting in a drop in eccentricity (supplementary). Accordingly, it is best to separate samples into distinct layers to reduce the risk of incorrectly measuring fibre orientations. Although there is no specific optimal thickness for use with SALS, above 800 μm, the fibre angles determined had very low eccentricity values, increasing the likelihood of extracting an incorrect mean angle. As a result, medial layer thicknesses below 600 μm were selected for testing in this study. Although layer separation was not carried out on previous arterial characterisation studies using SALS (Williams et al., 2009), the present study has identified it as an important consideration, particularly for larger mammalian arteries.

Additionally, collagen crimp which can be incorporated into constitutive models of collagenous tissues, for example (Tonge et al., 2015), is not explicitly recorded by SALS unlike techniques such as SHG (Chen et al., 2011; Haskett et al., 2013; Schrauwen et al., 2012).

Finally, this study has used SALS to identify fibre orientation in the circumferential-axial plane and is not well-suited for imaging radially orientated collagen fibres. While radial

fibres are not an important determinant for the pressure-diameter relationship of arteries, their number and density have been shown to be important in resisting delamination of arterial layers (Pal et al., 2014).

4.1.6 Conclusion

By comparing with accepted histological image processing results, this study has identified the optimum SALS setup for analysing the fibre architecture of large mammalian arteries and this same set-up can now be used for future studies on a range of similar sized vessels. SALS has been found to be a quick and easy method of accurately characterising collagen fibre orientation, particularly for intimal and medial arterial tissue, even when intact. Although SALS is less accurate in analysing the outer adventitial layer, the media is the most mechanically relevant layer in normal physiological vessel environments. SALS offers the unique ability to investigate real time load-induced reorganisation and remodelling of intact intima and media of arteries, thereby, offering a means to gain crucial insights into arterial disease.

Acknowledgements

The authors would like to acknowledge Thomas Sinnott, James Barry and Paul Normoyle for their help in setting up the system. This publication has emanated from research conducted with the financial support of the Irish Research Council (GOIPG/2014/515), Science Foundation Ireland under the Grant Number SFI/13/ERC/B2775 and the European Research Council (ERC) under the European Union's Horizon 2020 research and innovation programme (grant agreement No. 637674)

References

Berens, P., 2009. CircStat : A MATLAB Toolbox for Circular Statistics. J. Stat. Softw. 31, 1–21. doi:10.18637/jss.v031.i10

Billiar, K., Sacks, M., 1997. A method to quantify the fiber kinematics of planar tissues under biaxial stretch. J. Biomech. 30, 753–756.

Canham, P.B., Finlay, H.M., Dixon, J.G., Boughner, D.R., Chen, A., 1989. Measurements from light and polarised light microscopy of human coronary arteries fixed at distending pressure. Cardiovasc. Res. 23, 973–982. doi:10.1093/cvr/23.11.973

Chai, C.-K., Akyildiz, A.C., Speelman, L., Gijsen, F.J.H., Oomens, C.W.J., van Sambeek, M.R.H.M., Lugt, A. van der, Baaijens, F.P.T., 2015. Local anisotropic mechanical properties of human carotid atherosclerotic plaques – Characterisation by micro-indentation and inverse finite element analysis. J. Mech. Behav. Biomed. Mater. 43, 59–68. doi:10.1016/j.jmbbm.2014.12.004

Chen, H., Liu, Y., Slipchenko, M.N., Zhao, X., Cheng, J.-X., Kassab, G.S., 2011. The layered structure of coronary adventitia under mechanical load. Biophys. J. 101, 2555–62. doi:10.1016/j.bpj.2011.10.043

Cicchi, R., Kapsokalyvas, D., De Giorgi, V., Maio, V., Van Wiechen, A., Massi, D., Lotti, T., Pavone, F.S., 2010. Scoring of collagen organization in healthy and diseased human dermis by multiphoton microscopy. J. Biophotonics 3, 34–43. doi:10.1002/jbio.200910062

Creane, A., Maher, E., Sultan, S., Hynes, N., Kelly, D.J., Lally, C., 2011. Prediction of fibre architecture and adaptation in diseased carotid bifurcations. Biomech. Model. Mechanobiol. 10, 831–843. doi:10.1007/s10237-010-0277-8

Dahl, S., Vaughn, M., Niklason, L., 2007. An ultrastructural analysis of collagen in tissue engineered arteries. Ann. Biomed. Eng. 35, 1749–55. doi:10.1007/s10439-007-9340-8

Ellsmere, J.C., Khanna, R.A., Michael Lee, J., 1999. Mechanical loading of bovine pericardium accelerates enzymatic degradation. Biomaterials 20, 1143–1150. doi:10.1016/S0142-9612(99)00013-7

Flamini, V., Creane, A.P., Kerskens, C.M., Lally, C., 2015. Imaging and finite element analysis: A methodology for non-invasive characterization of aortic tissue. Med. Eng. Phys. 37, 48–54. doi:10.1016/j.medengphy.2014.10.006

Flamini, V., Kerskens, C., Moerman, K.M., Simms, C.K., Lally, C., 2010. Imaging Arterial Fibres Using Diffusion Tensor Imaging—Feasibility Study and Preliminary Results. EURASIP J. Adv. Signal Process. 2010, 1–14. doi:10.1155/2010/904091

Flamini, V., Kerskens, C., Simms, C., Lally, C., 2013. Fibre orientation of fresh and frozen porcine aorta determined non-invasively using diffusion tensor imaging. Med. Eng. Phys. 35, 765–776. doi:10.1016/j.medengphy.2012.08.008

Fomovsky, G.M., Holmes, J.W., 2010. Evolution of scar structure, mechanics, and ventricular function after myocardial infarction in the rat. AJP Hear. Circ. Physiol. 298, H221–H228. doi:10.1152/ajpheart.00495.2009

Gasser, T.C., Gallinetti, S., Xing, X., Forsell, C., Swedenborg, J., Roy, J., 2012. Spatial orientation of collagen fibers in the abdominal aortic aneurysm's wall and its relation to wall mechanics. Acta Biomater. 8, 3091–3103. doi:10.1016/j.actbio.2012.04.044

Gasser, T.C., Ogden, R.W., Holzapfel, G.A., 2006. Hyperelastic modelling of arterial layers with distributed collagen fibre orientations. J. R. Soc. Interface 3, 15–35. doi:10.1098/rsif.2005.0073

Gaul, R., Lally, C., 2017. Strain Mediated Enzyme Degradation of Arterial Tissue; Implications in Disease and Medical Device Design, in: Summer Biomechanics, Bioengineering and Biotransport Conference 2017. Tucson.

Ghazanfari, S., Driessen-Mol, A., Bouten, C.V.C., Baaijens, F.P.T., 2016. Modulation of collagen fiber orientation by strain-controlled enzymatic degradation. Acta Biomater. 35, 118–126. doi:10.1016/j.actbio.2016.02.033

Ghazanfari, S., Driessen-Mol, A., Strijkers, G.J., Baaijens, F.P.T., Bouten, C.V.C., 2015. The

Evolution of Collagen Fiber Orientation in Engineered Cardiovascular Tissues Visualized by Diffusion Tensor Imaging. PLoS One 10, e0127847. doi:10.1371/journal.pone.0127847

Ghazanfari, S., Driessen-Mol, a., Strijkers, G.J., Kanters, F.M.W., Baaijens, F.P.T., Bouten, C.V.C., 2012. A comparative analysis of the collagen architecture in the carotid artery: Second harmonic generation versus diffusion tensor imaging. Biochem. Biophys. Res. Commun. 426, 54–58. doi:10.1016/j.bbrc.2012.08.031

Haskett, D., Azhar, M., Utzinger, U., Vande Geest, J.P., 2013. Progressive alterations in microstructural organization and biomechanical response in the ApoE mouse model of aneurysm. Biomatter 3, e24648. doi:10.4161/biom.24648

Haskett, D., Johnson, G., Zhou, A., Utzinger, U., Vande Geest, J., 2010. Microstructural and biomechanical alterations of the human aorta as a function of age and location. Biomech. Model. Mechanobiol. 9, 725–736. doi:10.1007/s10237-010-0209-7

Holzapfel, G.A., Sommer, G., Auer, M., Regitnig, P., Ogden, R.W., 2007. Layer-Specific 3D Residual Deformations of Human Aortas with Non-Atherosclerotic Intimal Thickening. Ann. Biomed. Eng. 35, 530–545. doi:10.1007/s10439-006-9252-z

Hu, J., Humphrey, J.D., Yeh, A.T., 2009. Characterization of engineered tissue development under biaxial stretch using nonlinear optical microscopy. Tissue Eng. Part A 15, 1553–64. doi:10.1089/ten.tea.2008.0287

Keyes, J.T., Haskett, D.G., Utzinger, U., Azhar, M., Vande Geest, J.P., 2011. Adaptation of a planar microbiaxial optomechanical device for the tubular biaxial microstructural and macroscopic characterization of small vascular tissues. J. Biomech. Eng. 133, 75001. doi:10.1115/1.4004495

Nierenberger, M., Fargier, G., Ahzi, S., R??mond, Y., 2015. Evolution of the three-dimensional collagen structure in vascular walls during deformation: An in situ mechanical testing

under multiphoton microscopy observation. Biomech. Model. Mechanobiol. 14, 693–702. doi:10.1007/s10237-014-0630-4

Niestrawska, J.A., Viertler, C., Regitnig, P., Cohnert, T.U., Sommer, G., Holzapfel, G.A., 2016. Microstructure and mechanics of healthy and aneurysmatic abdominal aortas: experimental analysis and modelling. J. R. Soc. Interface 13, 20160620. doi:10.1098/rsif.2016.0620

O'Connell, M.K., Murthy, S., Phan, S., Xu, C., Buchanan, J., Spilker, R., Dalman, R.L., Zarins, C.K., Denk, W., Taylor, C.A., 2008. The three-dimensional micro- and nanostructure of the aortic medial lamellar unit measured using 3D confocal and electron microscopy imaging. Matrix Biol. 27, 171–81. doi:10.1016/j.matbio.2007.10.008

O'Rourke, M., 1995. Mechanical Principles in Arterial Disease. Hypertension 26, 2–9. doi:10.1161/01.HYP.26.1.2

Pal, S., Tsamis, A., Pasta, S., D'Amore, A., Gleason, T.G., Vorp, D.A., Maiti, S., 2014. A mechanistic model on the role of "radially-running" collagen fibers on dissection properties of human ascending thoracic aorta. J. Biomech. 47, 981–988. doi:10.1016/j.jbiomech.2014.01.005

Qi, N., Gao, H., Ogden, R.W., Hill, N.A., Holzapfel, G.A., Han, H.-C., Luo, X., 2015. Investigation of the optimal collagen fibre orientation in human iliac arteries. J. Mech. Behav. Biomed. Mater. 52, 108–119. doi:10.1016/j.jmbbm.2015.06.011

Rezakhaniha, R., Agianniotis, a., Schrauwen, J.T.C., Griffa, a., Sage, D., Bouten, C.V.C., Van De Vosse, F.N., Unser, M., Stergiopulos, N., 2012. Experimental investigation of collagen waviness and orientation in the arterial adventitia using confocal laser scanning microscopy. Biomech. Model. Mechanobiol. 11, 461–473. doi:10.1007/s10237-011-0325-z

Robitaille, M.C., Zareian, R., Dimarzio, C. a, Wan, K.-T., Ruberti, J.W., 2011. Small-angle

light scattering to detect strain-directed collagen degradation in native tissue. Interface Focus 1, 767–76. doi:10.1098/rsfs.2011.0039

Sacks, M.S., 2003. Incorporation of Experimentally-Derived Fiber Orientation into a Structural Constitutive Model for Planar Collagenous Tissues. J. Biomech. Eng. 125, 280–287. doi:10.1115/1.1544508

Sacks, M.S., Chuong, C.J.C., More, R., 1994. Collagen Fiber Architecture of Bovine Pericardium. ASAIO J. 40, M632–M637. doi:10.1097/00002480-199407000-00075

Sacks, M.S., Smith, D.B., Hiester, E.D., 1997. A small angle light scattering device for planar connective tissue microstructural analysis. Ann. Biomed. Eng. 25, 678–89.

Sáez, P., García, A., Peña, E., Gasser, T.C., Martínez, M.A., 2016. Microstructural quantification of collagen fiber orientations and its integration in constitutive modeling of the porcine carotid artery. Acta Biomater. 33, 183–193. doi:10.1016/j.actbio.2016.01.030

Schneider, C. a, Rasband, W.S., Eliceiri, K.W., 2012. NIH Image to ImageJ: 25 years of image analysis. Nat. Methods 9, 671–675. doi:10.1038/nmeth.2089

Schrauwen, J.T.C., Vilanova, A., Rezakhaniha, R., Stergiopulos, N., van de Vosse, F.N., Bovendeerd, P.H.M., 2012. A method for the quantification of the pressure dependent 3D collagen configuration in the arterial adventitia. J. Struct. Biol. 180, 335–42. doi:10.1016/j.jsb.2012.06.007

Schriefl, A.J., Zeindlinger, G., Pierce, D.M., Regitnig, P., Holzapfel, G.A., 2012. Determination of the layer-specific distributed collagen fibre orientations in human thoracic and abdominal aortas and common iliac arteries. J. R. Soc. Interface 9, 1275–86. doi:10.1098/rsif.2011.0727

Shahid, S.S., Kerskens, C., Gaul, R., Flamini, V., Lally, C., 2016. Ex-vivo arterial collagen fibre tractography using micro diffusion tensor imaging, in: ESMRMB 2016, 33rd Annual Scientific Meeting, Vienna, AT, September 29–October 1. Springer, Vienna, p. 28.

doi:10.1007/s10334-016-0568-x

Tonge, T.K., Ruberti, J.W., Nguyen, T.D., 2015. Micromechanical Modeling Study of Mechanical Inhibition of Enzymatic Degradation of Collagen Tissues. Biophys. J. 109, 2689–2700.

Tsamis, A., Krawiec, J.T., Vorp, D. a, 2013. Elastin and collagen fibre microstructure of the human aorta in ageing and disease: a review. J. R. Soc. Interface 10, 20121004–20121004. doi:10.1098/rsif.2012.1004

Voytik-Harbin, S.L., Roeder, B.A., Sturgis, J.E., Kokini, K., Robinson, J.P., 2003. Simultaneous mechanical loading and confocal reflection microscopy for three-dimensional microbiomechanical analysis of biomaterials and tissue constructs. Microsc. Microanal. 9, 74–85. doi:10.1017/S1431927603030046

Watson, S.R., Liu, P., Peña, E.A., Sutton, M.A., Eberth, J.F., Lessner, S.M., 2016. Comparison of Aortic Collagen Fiber Angle Distribution in Mouse Models of Atherosclerosis Using Second-Harmonic Generation (SHG) Microscopy. Microsc. Microanal. 22, 55–62. doi:10.1017/S1431927615015585

Williams, C., Liao, J., Joyce, E.M., Wang, B., Leach, J.B., Sacks, M.S., Wong, J.Y., 2009. Altered structural and mechanical properties in decellularized rabbit carotid arteries. Acta Biomater. 5, 993–1005. doi:10.1016/j.actbio.2008.11.028

Wolinsky, H., Glagov, S., 1964. Structural Basis for the Static Mechanical Properties of the Aortic Media. Circ. Res. 14, 400–413. doi:10.1161/01.RES.14.5.400

Wyatt, K.E.-K., Bourne, J.W., Torzilli, P. a, 2009. Deformation-Dependent Enzyme Mechanokinetic Cleavage of Type I Collagen. J. Biomech. Eng. 131, 51004. doi:10.1115/1.3078177

Zoumi, A., Lu, X., Kassab, G.S., Tromberg, B.J., 2004. Imaging Coronary Artery Microstructure Using Second-Harmonic and Two-Photon Fluorescence Microscopy.

Biophys. J. 87, 2778–2786. doi:10.1529/biophysj.104.042887

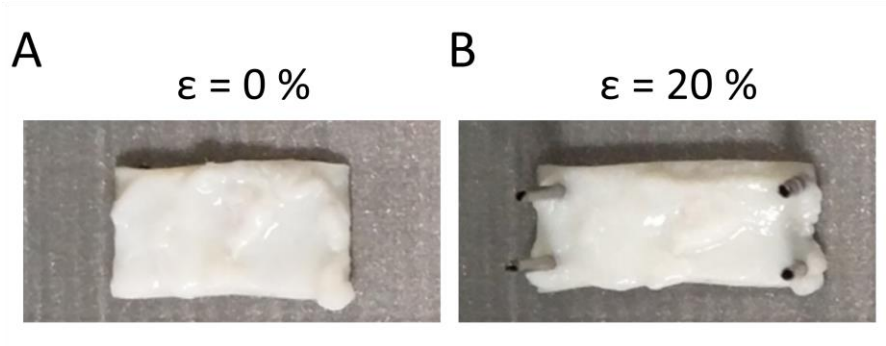

Figure 1 – Planar section of carotid artery in (A) the unloaded configuration and (B) the loaded pinned configuration.

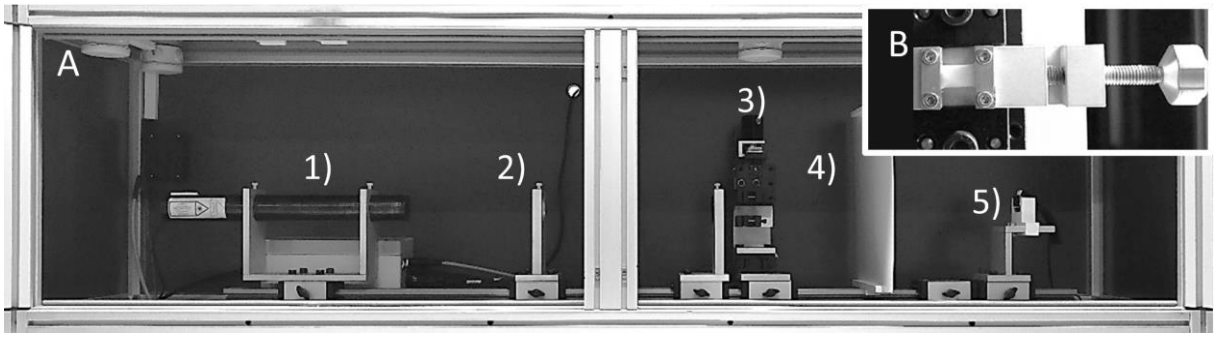

Figure 2 – (A) SALS setup consisting of 1) an unpolarised 5mW HeNe laser, 2) focusing lens, 3) automated sample positioner, 4) scatter plate and 5) CMOS camera, with (B) custom stretching device inset.

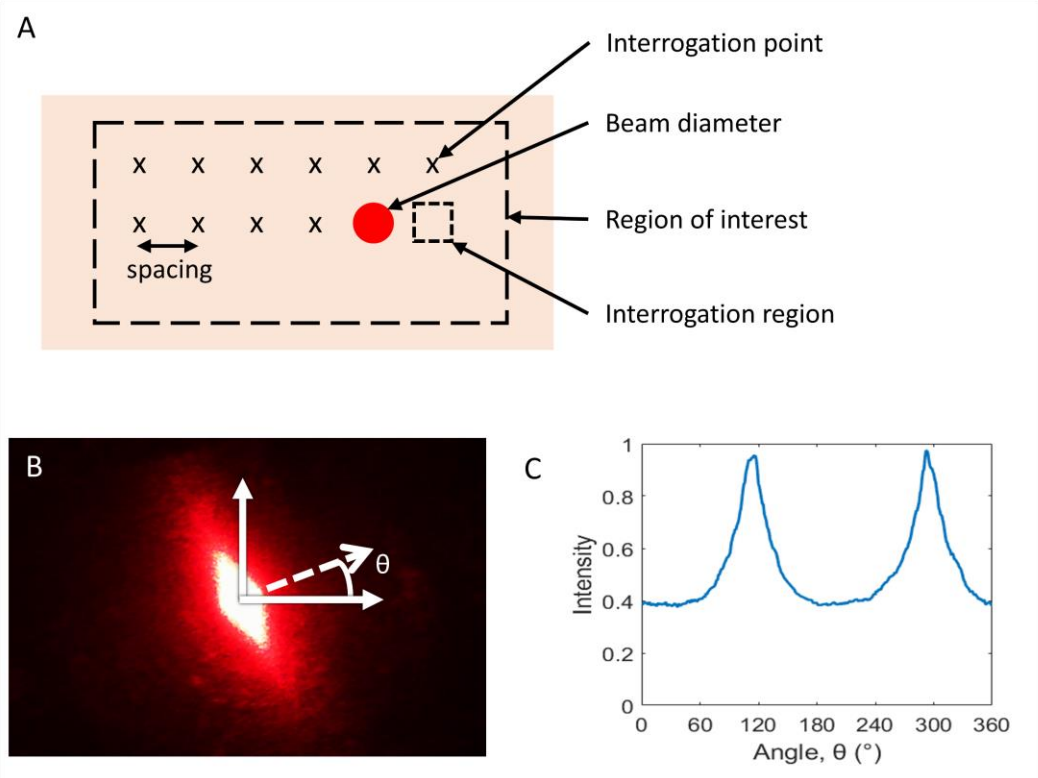

Figure 3 – (A) Schematic of a sample illustrating the key parameters in SALS analysis, (B) SALS pattern for single carotid artery location showing mean fibre direction overlaid which occurs orthogonally to angle of greatest light intensity shown in (C).

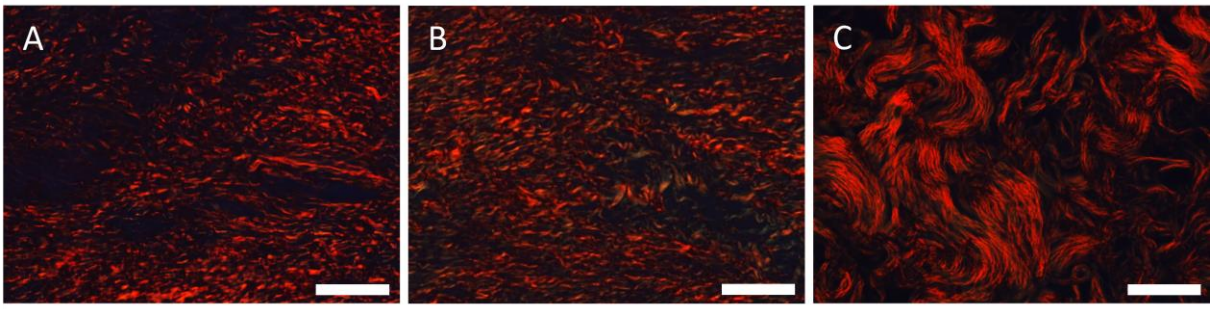

Figure 4 – Polarised light images of picrosirius red stained histological slices of (A) intima, (B) media and (C) adventitia showing layer specific fibre architecture. Scale bar: 50 μm.

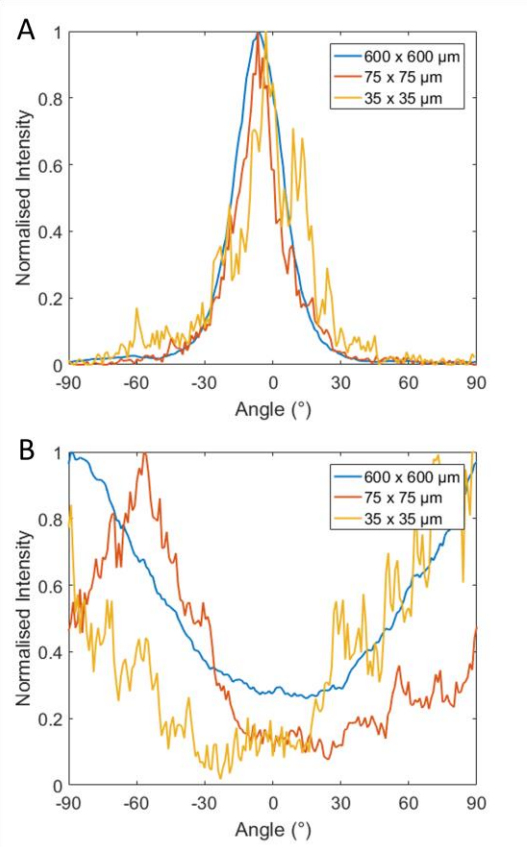

Figure 5 – HOA fibre orientation results for interrogation region area of 35 x 35 µm, 75 x 75 µm and 600 x 600 µm for (A) media and (B) adventitia showing effect of interrogation area for specific layers.

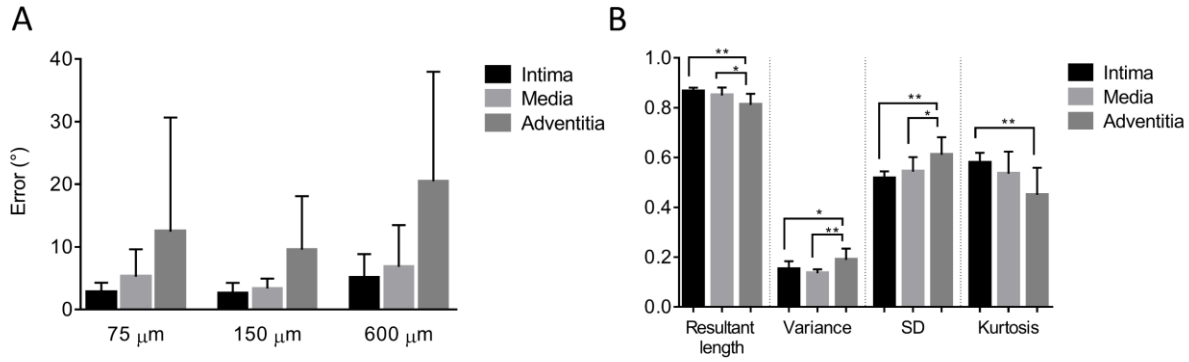

Figure 6 – (A) Angular error between SALS and HOA results for different beam diameters. (B) circular statistical analysis highlighting different architecture of the adventitia with a 150 µm interrogation region. n=10, *p<0.05, **p<0.01.

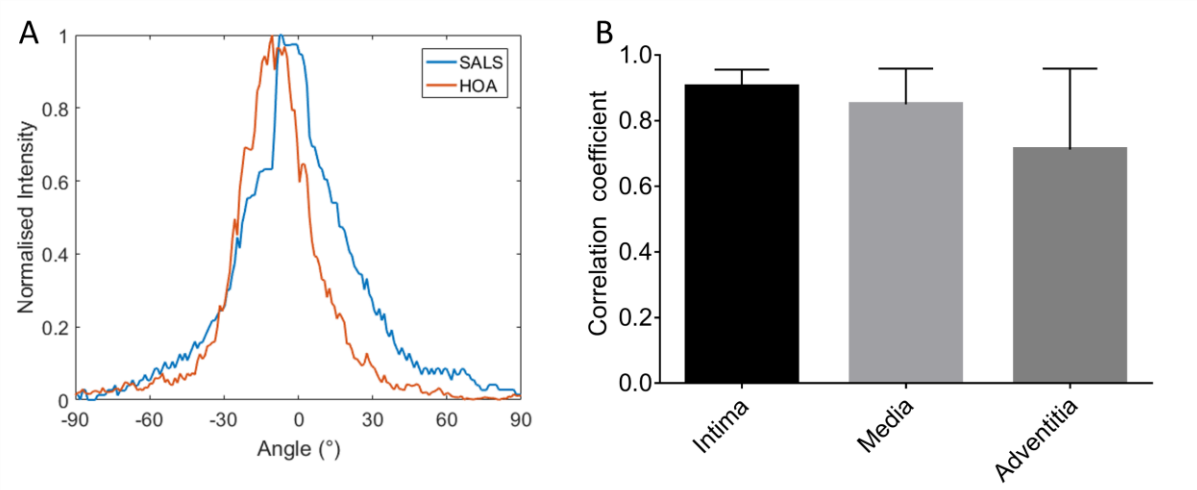

Figure 7 – (A) Medial fibre distribution determined using SALS and HOA for the same location, (B) Correlation coefficients between SALS and HOA for each layer. n=10.

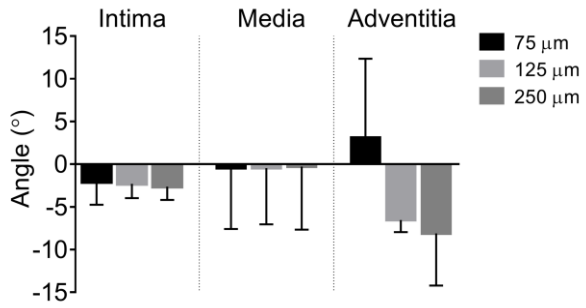

Fig. 8 – Mean fibre angle measured using SALS across each layer using different interrogation spacing sizes. For interrogation point spacings of 75 µm, 125 µm, 250 µm, the total number of interrogation points are 600, 288 and 72 respectively.

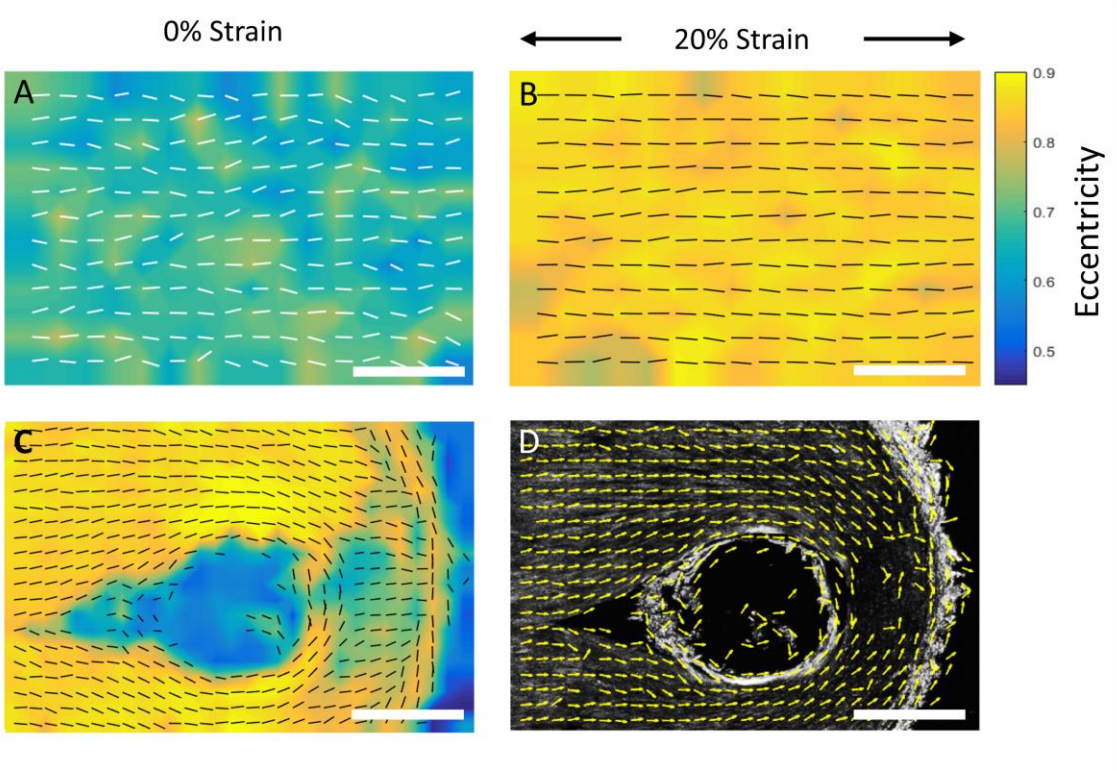

Figure 9 – Representative vector map of fibre directions overlaid on a contour plot of scattered light eccentricity produced using SALS for (A) unstretched media, (B) stretched media,(C) around the pinned region of tissue and(D) vector map of the same pinned location showing similar fibre patterns produced using HOA. Scale bar: 1000 μm.

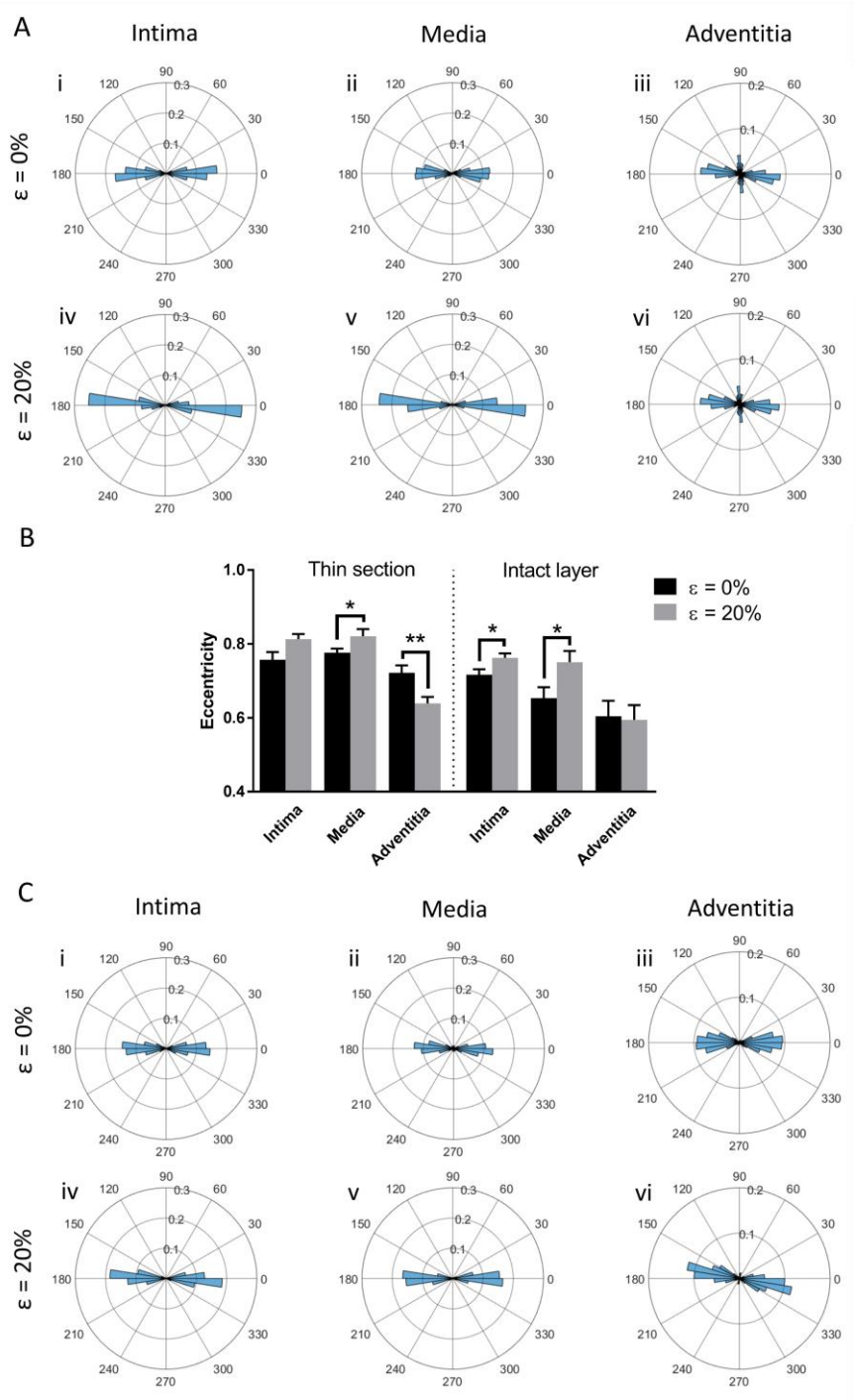

Figure 10 – (A) Polar histogram plot of fibre distribution of histological sections (n = 9) under i-iii) 0% strain and iv-vi) 20% strain. (B) Eccentricity results for histological sections (n = 9) and intact layers (n = 6) in the unloaded and loaded configuration. (C) Polar histogram plot of fibre distribution of intact layers (n = 6) under i-iii) 0% strain and iv-vi) 20% strain. Each sample is made up of 1152 interrogation points. *p<0.05, **p<0.01.